Available online at www.sciencedirect.com
ScienceDirect
Electrochemistry Communications 10 (2008) 625–629
electrochemistry communications
www.elsevier.com/locate/elecom

Self-assembled synthesis of SERS-active silver dendrites and photoluminescence properties of a thin porous silicon layer

Weichun Ye [a,b], Chengmin Shen [a], Jifa Tian [a], Chunming Wang [b,*], Lihong Bao [a], Hongjun Gao [a,*]

[a] *Beijing National Laboratory for Condensed Matter Physics, Institute of Physics, Chinese Academy of Sciences, Beijing 100080, China*
[b] *Department of Chemistry, Lanzhou University, Lanzhou 730000, China*

Received 8 December 2007; received in revised form 18 January 2008; accepted 31 January 2008
Available online 8 February 2008

Abstract

Via electroless metal deposition, well-defined silver dendrites and thin porous silicon (por-Si) layers are simultaneously prepared in ammonia fluoride solution containing $AgNO_3$ at 50 °C. A self-assembled localized microscopic electrochemical cell model and a diffusion-limited aggregation mode are used to explain the growth of silver dendrites. The formation of silver dendritic nanostructures derives from the continuous aggregation growth of small particles on a layer of silver nanoparticles or nanoclusters (Volmer-Weber layer). Thin and homogeneous nanostructure por-Si layers display visible light-emission properties at room temperature. The investigation of the surface-enhanced Raman scattering (SERS) reveals that the film of silver dendrites on por-Si is an excellent substrate with significant enhancement effect.

Keywords: Electroless deposition; Silver dendrites; Thin porous silicon; Photoluminescence; Surface-enhanced Raman scattering (SERS)

1. Introduction

A great deal of effort has been made to fabricate well-defined nanostructured noble metals such as nanoparticles, nanorods, and nanowires due to their unique optical, electronic, catalytic properties, and surface-enhanced Raman scattering (SERS) [1–4]. The intrinsic properties of the noble metal nanostructure are determined by its size, shape, morphology, composition, and crystallinity [5]. Recently, researchers [6–9] have developed a simple electroless metal deposition (EMD) method in a HF solution containing $AgNO_3$ to synthesize unique silver dendritic nanostructures with stems, branches, and leaves, and simultaneously form large-area silicon nanowire arrays on the silicon substrates.

EMD in ionic metal (silver) HF solution is based on an electrochemical redox reaction in which both anodic and cathodic processes occur simultaneously at the silicon surface [10]. Electrochemical reactions are illustrated in the following equations. All potentials refer to the standard hydrogen electrode (SHE).

$$\text{Anodic}: \quad Si + 6HF \rightarrow H_2SiF_6 + 4H^+ + 4e \qquad E = -1.24\ \text{V} \tag{1}$$

$$\text{Cathodic}: \quad Ag^+ + e \rightarrow Ag \qquad E = +0.80\ \text{V} \tag{2}$$

Since Si nanostructures have unusual properties such as single-electron tunneling, nonlinear optical properties and visible photoluminescence (PL) [11–13], turning bulk Si into nanocrystals or nanocrystalline networks is very interesting. Electroless etching of Si to form por-Si is a simple process that requires the attachment of no electrodes and can be performed on objects of arbitrary shape and size. Nonetheless, the formation of por-Si via electroless etching

* Corresponding authors.
E-mail addresses: wangcm@lzu.edu.cn (C. Wang), hjgao@aphy.iphy.ac.cn (H. Gao).

1388-2481/$ - see front matter © 2008 Elsevier B.V. All rights reserved.
doi:10.1016/j.elecom.2008.01.040

has received much less systematic investigation [14,15]. To date, the preponderance of work has concentrated on the use of HF solution. However, according to our understanding on the electrochemical redox reaction process and the fact that a highly concentrated NH_4F solution is still necessary as a silicon oxide etchant for patterning the oxidized surfaces, we believe that the use of a wider range of fluoride carriers can lead to a greater control over morphology and properties. Herein, we show in detail the formation of silver dendritic nanostructures and a thin por-Si layer via an EMD process based on NH_4F–$AgNO_3$ system. The growth evolution mechanism of silver dendrites was also discussed. Then the SERS spectra of Rhodamine B (RB) on silver dendritic nanostructures were demonstrated, which reflected the different SERS effects based on different size and amount of Ag dendrites. In addition, the thin homogeneous por-Si layer was demonstrated to have an intensive visible-light emitting property.

2. Experimental

Silver nitrate was purchased from Acros, RB was obtained from Sigma. All reagents and solvents were used without further treatment. Double distilled water was used through the experiments.

The p-type silicon (1 1 1) wafers were cleaned with acetone and ethanol to remove possible contaminants, and then etched in a 5 wt% HF solution for 10 min to remove the native oxide layer. The wafers were rinsed with water and dried with dry nitrogen flux after each cleaning step. Subsequently, the cleaned silicon wafers were immersed in a 2.5 M NH_4F solution containing 0.01 M silver nitrate at 50 °C for different times. After the etching process, the silicon wafers were rinsed with water and blown dry by air.

A field-emission-type scanning electron microscope (FE-SEM; Model XL-SFEG; FEI Corp.) and an atomic force microscope (AFM, in tapping mode; Nanoscope III a, DI. Cop. Ltd.) were used to observe the morphologies of the samples. PL measurement was performed at room temperature on a Reinshaw Raman spectrometer by using a He–Cd laser as the excitation light source with the wavelength of 325 nm.

RB molecules were used to test the enhancement ability of the SERS active substrates. The as-prepared silver films on silicon substrates were soaked in a 10^{-4} M aqueous RB solution for 30 min, taken out, and rinsed using water for three times. The Raman scattering measurements were performed at room temperature on a Raman system (JY-HR800) with confocal microscopy. The solid-state diode laser (633 nm) was used as an excitation source. The laser power on the samples was kept with 0.9 mW and the typical spectrum acquisition time was 50 s. The probed area was about 1 μm in diameter with a 50x microscope objective lens.

3. Results and discussion

In NH_4F solution, the etched silicon substrates were always wrapped with a layer of thick silver film, which is rather loose and can be easily detached from the surface

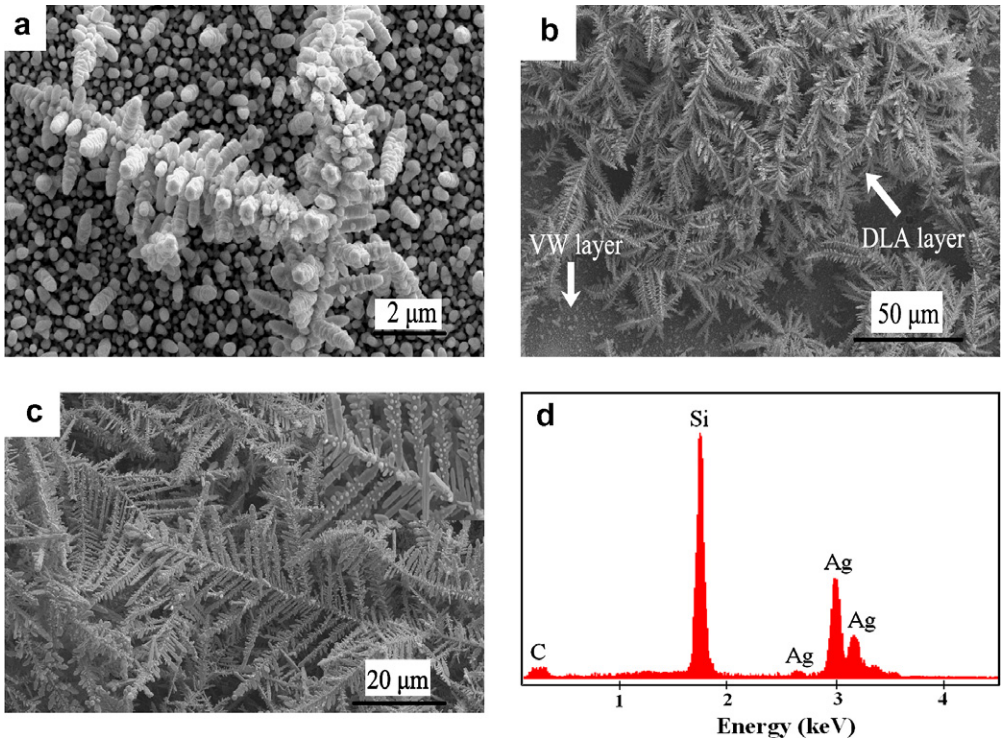

Fig. 1. SEM images of the silver films prepared in a 2.5 M NH_4F solution containing 0.01 M silver nitrate at 50 °C for 5(a), 15(b) and 60(c) min; (d) EDX spectrum of the VW layer in (b). The inset of (c) shows large-magnification SEM image.

of silicon substrates. A morphological evolution of silver dendrites was followed by a time-dependent process. Fig. 1a–c shows the SEM images of silver films prepared in the solution of 0.01 M $AgNO_3$ + 2.5 M NH_4F for 5, 15, and 60 min, respectively. At 5 min, silver nanoparticles or nanoclusters were formed. As time went on, the silver nanoparticles tend to aggregate and finally self-assembled to form silver dendrites. Well-defined dendritic structure was arranged along a backbone with symmetrical side-branches. As the reaction time proceeded, more and more silver dendrites stacked on the surface, and an interesting phenomenon is that some "new" branches have grown on the "old" branches (Fig. 1c).

NH_4F is a salt consisting of a weak acid with a weak base group. The equilibrium constant can be calculated from the reaction [16]:

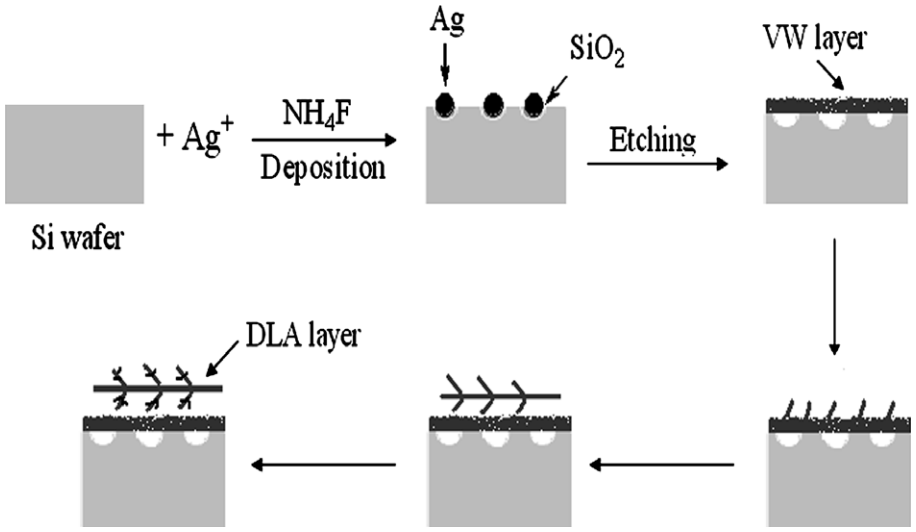

Fig. 2. Schematic illustration of the growth process of silver dendrites.

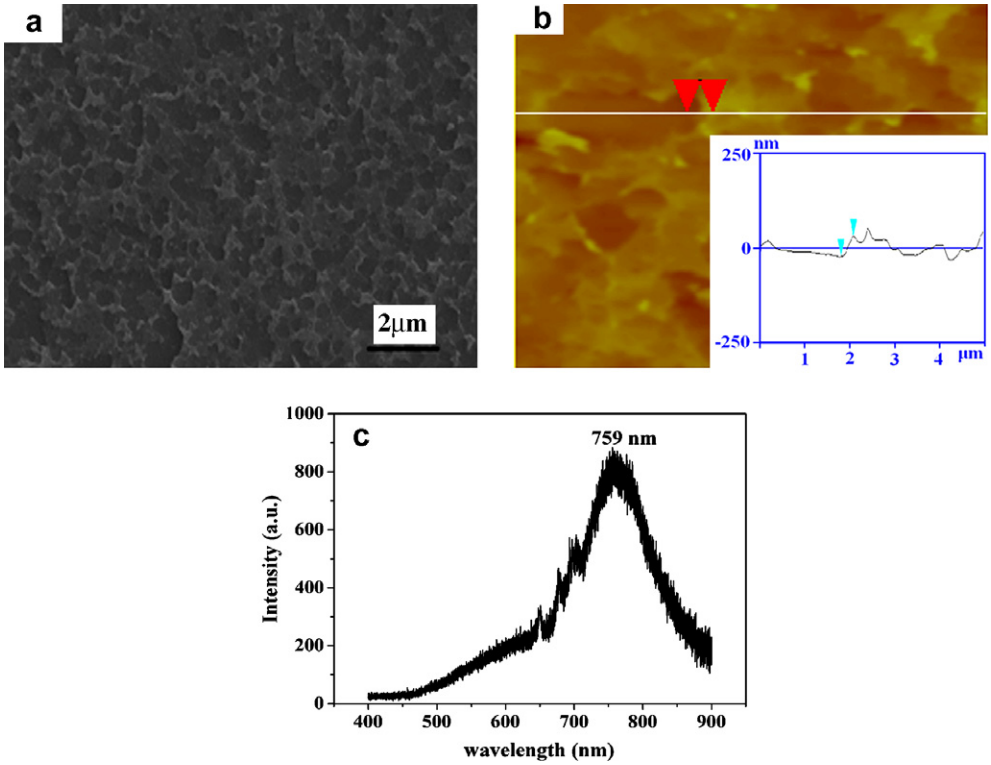

Fig. 3. SEM image of the thin por-Si layer (a) and its 2D AFM surface analysis in vertical distance (b); (c) is the corresponding PL spectrum.

$$NH_4^+ + F^- \Longleftrightarrow NH_3 + HF \quad (3)$$

$$K = K_a(NH_4^+)/K_a(HF) \approx 10^{-6} \quad (4)$$

The concentration of free HF is about 10^{-2} M in this solution with the pH value of 7.8. From the Nernst equation, the anodic potential difference between the NH_4F–$AgNO_3$ solution and HF–$AgNO_3$ solution under the identical conditions can be easily written by the following:

$$\Delta E = -0.0591 g K^{\frac{1}{2}} = \frac{-0.059}{2} 1g(10^{-6}) = 0.177\ V \quad (5)$$

Therefore, the electroless silver deposition in NH_4F solution is thermodynamically favored. The formation of the silver dendritic nanostructures can be also understood on the basis of self-assembled localized microscopic electrochemical cell model and diffusion-limited aggregation process (DLA) [7,17]. Through the morphological evolution of silver dendritic nanostructures, Fig. 2 gives a more detailed schematic illustration of formation process of silver dendrites than the previously proposed mechanisms [7–9]. Here, the layer of silver nanoparitcles or nanoclusters and the layer of the synchronized silver dendrites were named as the Volmer-Weber (VW) layer and the DLA layer, respectively. It is assumed that the DLA layer derived from the continuous aggregation growth of small particles on the VW layer, as shown in Fig. 1b. Fig. 1d shows the energy-dispersive X-ray (EDX) spectrum, which corresponds to the VW layer of Fig. 1b. This provides direct proof that these particles on the silicon substrate are silver. In fact, the case of HF–$AgNO_3$ system is also similar to this work, while the formation rate of VW layer is faster in the HF–$AgNO_3$ system, which might be attributed to the drop of surface energy due to the increased HF concentration [18].

Fig. 3a shows the SEM image of a thin por-Si layer, which was etched in 2.5 M NH_4F solution containing 0.01 M silver nitrate at 50 °C for 60 min, detached the silver film, and then immersed into a 50% HNO_3 solution for 30 min. It can be seen that the por-Si layer is nanoporous and thin with homogenous "pits". Its 2D AFM surface analysis in vertical distance shows a thickness of about 54 nm (Fig. 3b).

The PL spectrum of the thin por-Si layer is shown in Fig. 3c. The material shows its visible light-emission property at room temperature with the PL peak at 759 nm. The mechanism of por-Si luminescence has not been completely understood up to date. The microstructure of light emitting por-Si plays an important role in this discussion since quantum confinement is one of the arguments [19]. Si–Ag bonds were formed through the Ag atoms combining with Si dangling bonds [20]. However, the Si–Ag bonds were not easily eliminated [21,22] via the treatment of HNO_3 solution. This would lead to somewhat changed PL. There is enough evidence to attribute the PL properties of these samples to the formation of thin por-Si simultaneous to (and as a result of) the synthesis of silver dendrites in fluoride media.

SERS application of the as-prepared silver deposits was subsequently evaluated using RB as probe molecules. Raman signals on a flat Si surface are very weak (Fig. 4d). Prior to the measurement, one drop of 10^{-3} M RB solution was dropped on the flat Si wafer and then

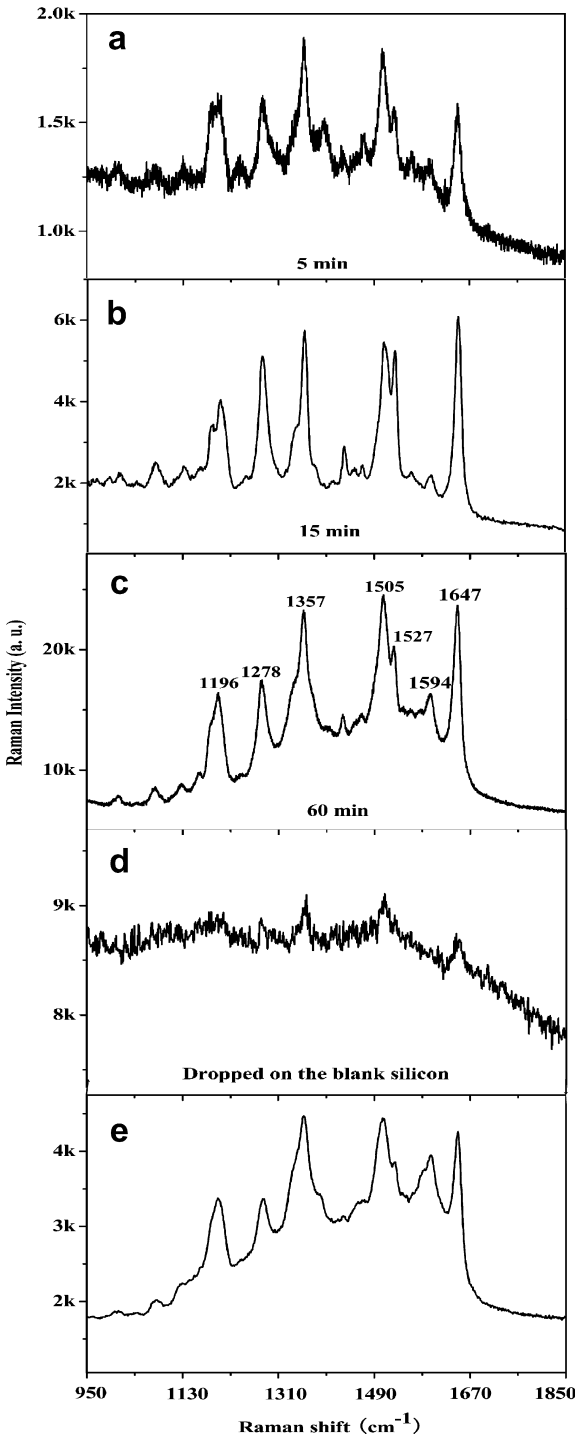

Fig. 4. SERS spectra acquired from RB of 10^{-4} M absorbed on the silver films prepared in NH_4F–$AgNO_3$ solution for 5(a), 15(b) and 60(c) min; (d) shows the Raman signals from the sample, which was obtained by dropping one drop of 10^{-3} M RB solution on a flat Si wafer and being dried in the air; (e) shows the Raman spectrum of RB from 10^{-5} M on the silver dendrites prepared in NH_4F–$AgNO_3$ solution for 60 min.

dried in the air. If the silver deposits on thin porous silicon wafer were prepared in NH_4F–$AgNO_3$ solution for different etched time as SERS substrates, enhanced characteristic features for RB were observed in Fig. 4a–c. To further demonstrate the variation in SERS efficiency with different deposition times, the Raman peak of 1647 cm^{-1} was chosen as the identification position. The SERS intensities corresponding to the silver films deposited on silicon for 15 min (Fig. 4b) and 60 min (Fig. 4c), respectively, show 9 and 25 times as strong as the film deposited for 5 min (Fig. 4a). Much research [23–26] demonstrated that dendritic nanostructures consist of numerous nanostructures whose distance is located in the range of effective plasma resonance, resulting in the amplification of the electromagnetic field and enhancement of the effective rate of polarization for adsorbed molecules; thus, enhancing the SERS activity with the deposition time can be attributed to the increasing amounts of silver dendrites, which is consistent with the SEM observations. As seen in Fig. 4e, the SERS spectrum of RB from a more diluted solution (10^{-5} M) still exhibits a high intensity. Such silver dendritic nanostructures supported on the thin por-Si surface are suitable for the Raman enhancement and exploit a wide way for Raman analysis and imaging.

4. Conclusions

In summary, we have demonstrated a simple method to the simultaneous formations of silver dendritic nanostructures and a thin porous silicon layer in ammonia fluoride solution. The morphology of the silver deposits at different deposition times shows that the formation of silver dendritic nanostructures derives from the continuous aggregation growth of small particles on the Volmer-Weber layer. The obtained thin and homogeneous por-Si layer displays a good visible photoluminescence. The SERS effect of the film of Ag dendrites through the adsorption of RB molecules indicates that the film of silver dendrites on por-Si is an active substrate for enhanced SERS signals.

Acknowledgment

This work was supported by the National Science Foundation of China under Grant Nos. 60571045 and 20577017.

References

[1] Y. Sun, Y. Xia, Science 298 (2002) 2176.
[2] F. Kim, J.H. Song, P.D. Yang, J. Am. Chem. Soc. 124 (2002) 14316.
[3] T. Teranishi, M. Miyake, Chem. Mater. 10 (1998) 594.
[4] A.M. Michaels, J. Jiang, L. Brus, J. Phys. Chem. B 104 (2000) 11965.
[5] R.C. Jin, C.Y. Cao, E.C. Hao, G.S. Métraux, G.C. Schatz, C.A. Mirkin, Nature 425 (2003) 487.
[6] K. Peng, Y. Yan, S. Gao, J. Zhu, Adv. Mater. 14 (2002) 1164.
[7] K. Peng, Y. Yan, S. Gao, J. Zhu, Adv. Funct. Mater. 13 (2003) 127.
[8] T. Qiu, X.L. Wu, Y.F. Mei, P.K. Chu, G.G. Siu, Appl. Phys. A 81 (2005) 669.
[9] T. Qiu, X.L. Wu, X. Yang, G.S. Huang, Z.Y. Zhang, Appl. Phys. Lett. 84 (2004) 3867.
[10] P. Gorostiza, M.A. Kulandainathan, R. Diaz, F. Sanz, P. Allongue, J.R. Morante, J. Electrochem. Soc. 14 (2000) 1026.
[11] L.T. Canham, Appl. Phys. Lett. 57 (1990) 1046.
[12] A.G. Cullis, L.T. Canham, Nature 353 (1991) 335.
[13] B.H. Choi, S.W. Hwong, I.G. Kim, H.C. Shin, Y. Kim, E.K. Kim, Appl. Phys. Lett. 73 (1998) 3129.
[14] A.G. Cullis, L.T. Canham, P.D.J. Calcott, J. Appl. Phys. 82 (1997) 909.
[15] L.A. Jones, G.M. Taylor, F.X. Wei, D.F. Thomas, Prog. Surf. Sci. 50 (1995) 283.
[16] M. Chemla, T. Homma, V. Bertagna, R. Erre, N. Kubo, T. Osaka, J. Electroanal. Chem. 559 (2003) 111.
[17] T.A. Witten, L.M. Sander, Phys. Rev. Lett. 47 (1981) 1400.
[18] W. Ye, Y. Chang, C. Ma, B. Jia, G. Cao, C. Wang, Appl. Surf. Sci. 253 (2007) 3419.
[19] P.D.J. Calcott, K.J. Nash, L.T. Canham, M.J. Kane, D. Brumhead, J. Phys. C 5 (1993) L91.
[20] M. Sakurai, C. Thirstrup, M. Aono, Phys. Rev. B 62 (2000) 16167.
[21] F. Jing, H. Tong, C. Wang, J. Solid State Electrochem. 8 (2004) 877.
[22] F.A. Harraz, T. Tsuboi, J. Sasano, T. Sakka, Y.H. Ogata, J. Electrochem. Soc. 149 (2002) C456.
[23] J. Zhang, X. Li, X. Sun, Y. Li, J. Phys. Chem. B 109 (2005) 12544.
[24] C. Jing, Y. Fang, J. Colloid Interface Sci. 314 (2007) 46.
[25] N.H. Kim, K. Kim, J. Raman Spectrosc. 36 (2005) 623.
[26] J. Jiang, K. Bosnick, M. Maillard, L. Brus, J. Phys. Chem. B 107 (2003) 9964.